



Article

# Finger-Ring Dielectric Resonator Antenna for Millimeter-Wave Applications

Tarek S. Abdou<sup>1\*</sup>, Rawad Asfour<sup>2</sup><sup>1</sup>Electrical and Electronic Engineering Department, Higher Institute of Engineering Technology-Tripoli, Libya<sup>2</sup>School of Computer and Electronic Engineering (CSEE), University of Essex, Essex, UK\*Corresponding author: [tsabdou1@hiett.edu.ly](mailto:tsabdou1@hiett.edu.ly)

Received: December 18, 2024

Accepted: December 25, 2024

Published: February 15, 2025

This is an open access article under the BY-CC license

**Abstract:** A mm-wave circularly polarized (CP) dielectric resonator antenna (DRA) for finger-worn applications is proposed, designed, and simulated. The proposed DRA utilizes a conformal configuration and operates within the 20–30 GHz frequency range. A cylindrical substrate supports a dielectric resonator with a relative permittivity. The antenna dimensions are 6 mm and 3.4 mm, with a conformal ground plane of 20 mm and 10 mm. The finger-ring DRA is tested in both free space and on-body situations. In on-body, the impedance bandwidth drops from 20% in free space to 15%, and the CP bandwidth drops from 12% to 3.5%. The off-body configuration achieves a peak gain of approximately 8 dBi, which decreases by approximately 1 dB in the on-body case. The radiation patterns and axial ratio demonstrate the suitability of the design for wearable applications. A comparative analysis with existing literature highlights the advantages of the proposed DRA in terms of bandwidth, gain, and polarization characteristics.

**Keywords:** Wearable antenna, circular polarization, dielectric resonator antenna, finger-ring antenna, mm-wave communication.

## 1. Introduction

Millimeter-wave (mmWave) antennas enable high-speed data transmission up to 10 Gbps with significantly larger bandwidths than microwave frequencies, which are limited to 1 Gbps [1]. Their adoption has accelerated with 5G, unlocking new multimedia applications despite challenges in achieving high gain, agile beamforming, and wide-scan capabilities [2]. Various designs address these challenges, including dual-polarized microstrip antennas with air cavities to reduce losses [3], wideband multi-circular loop antennas with high efficiency [4], and dual-band arrays enhancing gain at 28 GHz and 38 GHz [5-7]. Beam-steering technologies such as phased arrays, quasi-optical systems, leaky-wave antennas, and metasurfaces improve adaptability for Beyond-5G and 6G networks [8].

Ultra-wideband designs enhance isolation and efficiency [9], while machine learning optimizes gain and bandwidth [10]. Wearable antennas are essential for Body-Centric Communication (BCC) in Wireless Body Area Networks (WBANs) for applications in healthcare, military, and sports [11]. These antennas operate near the human body, with performance influenced by factors like return loss, gain, bandwidth, and radiation pattern. The design of wearable antennas must address challenges such as compactness, flexibility, and resistance to mechanical deformations [12].

With the rise of 5G and 6G technologies, wearable antennas are evolving to meet demands for high data rates and low power consumption [13]. Approaches like metamaterials and the use of textile or nanomaterials improve efficiency and radiation performance [14,15]. Wearable antennas also find applications in wireless power transmission (WPT) for IoT devices [16], real-time health monitoring

[17], and Bluetooth/Wi-Fi communication [18]. These advancements emphasize the role of wearable antennas in enabling reliable and efficient connectivity [19,20].

Wearable finger-ring antennas have gained significant attention in body-centric wireless communication due to their compactness, flexibility, and suitability for applications such as health monitoring, IoT, and 5G/mmWave communications. Various designs have been introduced, each targeting specific frequency bands and functionalities. A microstrip patch antenna mounted on a gold base was developed for body-centric wireless sensor networks at 5 GHz, achieving a peak gain of 6.9 dBi and a -10 dB bandwidth of 90.3 MHz [21].

A conformal loop antenna supporting ISM, LTE, WiMAX, and 5G bands demonstrated reliable performance at a 3 mm spacing from the finger, with an indoor operational range exceeding 8.6 meters [22]. A dual-finger ring antenna was designed for UWB applications (7.25–10.25 GHz), ensuring minimal interference from the human finger [23]. For medical sensing, a miniaturized antenna operating at the 2.45 GHz ISM band was proposed, featuring low SAR and a compact form factor for everyday use [24]. The effect of finger positioning and rotation on a dual-band inverted-F antenna for BAN applications (2.4–2.5 GHz and 915–930 MHz) was analyzed, highlighting variations in VSWR due to orientation changes [25]. A UHF RFID tag antenna for secure environments and healthcare applications exhibited read distances ranging from 2 to 5 meters based on substrate height [26].

Additionally, a 28 GHz finger-ring antenna array for mmWave 5G applications was developed, achieving a peak gain of 5.14 dBi with a miniaturized structure [27]. These advancements demonstrate the increasing versatility of wearable finger-ring antennas in modern wireless systems. Despite these advancements, finger-worn dielectric resonator antennas (DRAs) have received limited attention, even though they outperform traditional microstrip-based designs in terms of efficiency, compactness, and polarization purity. Moreover, DRAs have already been designed and tested for both off-body [28] and on-body [29] applications in the mmWave band.

This study introduces a novel circularly polarized (CP) finger-ring dielectric resonator antenna (DRA) operating in the 20–30 GHz range, designed to address the growing demand for high-performance mmWave wearable antennas. Compared to existing finger-worn antennas [21–27]. This work offers distinct advantages by introducing a compact CP-DRA for mmWave applications, addressing a critical gap in wearable antenna technology. The proposed design demonstrates enhanced efficiency, polarization purity, and robustness, outperforming conventional finger-worn antennas. The performance of the proposed design is evaluated under both free-space and on-body conditions to assess its practical viability. The results provide significant insights into the integration of DRAs into compact wearable devices, paving the way for advancements in communication and healthcare technologies.

## 2. Antenna configuration

The proposed finger-ring Dielectric Resonator Antenna (DRA) is illustrated in Figure 1. The design incorporates a rectangular dielectric resonator, strategically mounted on a curved substrate with a conformal ground plane to enhance its performance when worn on the finger. The ring substrate, which is the core component of the antenna, features a radius of 10 mm and a thickness of 0.3 mm, chosen to ensure compactness while maintaining efficient radiation properties at the targeted mm-wave frequencies. Table 1 illustrates the Antenna parameters.

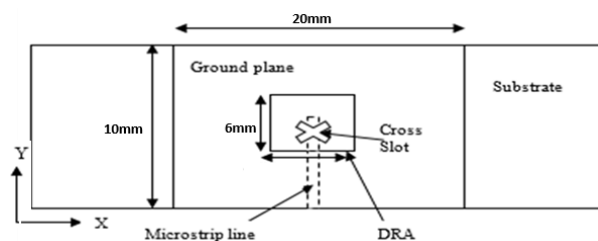


Figure 1. The proposed ring-DRA.

The antenna structure is designed to be both lightweight and flexible, adhering to the anatomical contours of the finger to provide a comfortable fit while optimizing performance. A key feature of this design is the excitation mechanism, which utilizes a slot-coupled feeding structure. This feeding mechanism has been selected to ensure efficient energy transfer to the dielectric resonator, enabling the antenna to achieve circularly polarized (CP) radiation. The use of CP radiation is particularly beneficial for wearable devices, as it improves the robustness of signal reception and transmission, especially in dynamic environments where the orientation of the device may change frequently.

**Table 1.** Dimensions of the Planar Configuration.

Component	Dimensions (mm)	Material	Properties
RDR	$l_1 = w_1 = 6, h_1 = 3.334$	Alumina (95.5%)	$\epsilon_{r1} = 9.9, \tan \delta = 0.0001$
Cylindrical Substrate	radius = 10, Thickness = 0.3	Roger Ro4003	$\epsilon_s = 3.5, \tan \delta = 0.0027$
Ground Plane	$L = 20, W = 10$	PEC (Perfect Electric Conductor)	—
Microstrip-Line	$l_t = 5, w_t = 0.32$	Copper (pure)	—
Cross Slot	$l_{s1} = 2, l_{s2} = 4, w_s = 0.43$	—	—

The conformal ground plane, designed to closely follow the curvature of the finger, plays a crucial role in maintaining a stable radiation pattern while minimizing the interaction between the antenna and the human body. This design ensures that the antenna can operate effectively in practical wearable applications, where consistent performance across a wide range of operating conditions is essential. The integration of these design features allows the proposed finger-ring DRA to maintain a small form factor while delivering efficient, high-performance operation for use in mm-wave communication systems. Ring DRA in free space and on the equivalent finger shows in [Figure 2](#).

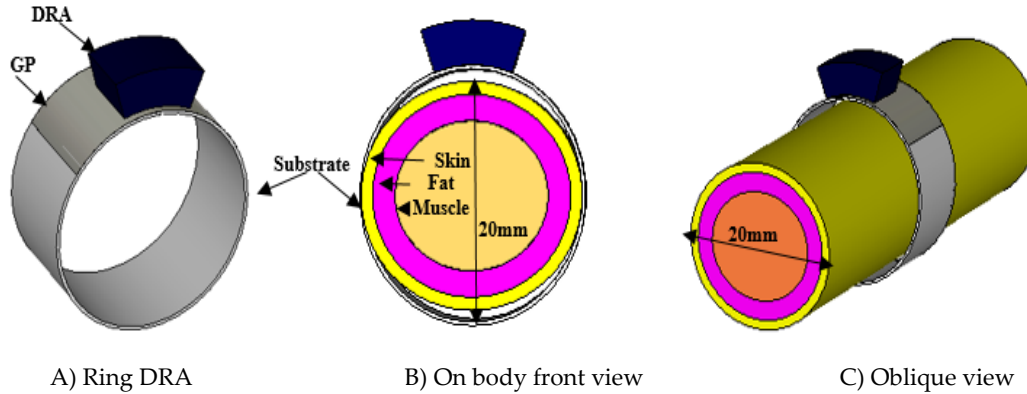


**Figure 2.** Ring DRA in free space and on the equivalent finger.

**Dielectric Constants: DRA:** The dielectric constant of the dielectric resonator (DRA) material is a critical factor influencing the resonant frequency and bandwidth of the antenna. For this design, the dielectric constant of the DRA material is carefully selected to ensure the antenna resonates efficiently within the 20–30 GHz operating frequency band. **Substrate:** The substrate material, on which the DRA is mounted, is chosen for its low loss, high flexibility, and suitable dielectric constant to support optimal antenna performance in wearable applications.

This choice helps minimize signal degradation and ensures effective radiation. **Antenna Dimensions:** The finger-ring DRA is compactly designed with dimensions of 6 mm x 6 mm x 3.4 mm, offering a small yet efficient form factor ideal for wearable applications. These dimensions are selected to enable the antenna to function effectively at the target mm-wave frequencies while remaining lightweight and comfortable when worn on the finger.

The antenna incorporates a 20 mm x 10 mm ground plane, which ensures proper impedance matching and is designed to shield the human body from unwanted electromagnetic radiation [30]. The

size of the ground plane is optimized to provide consistent performance across the operating frequency range while minimizing interference from the human body during practical use. Operating frequency: The antenna operates within the 20–30 GHz frequency band, which is ideal for high-frequency communication systems, including emerging 5G and future wireless technologies.

The high-frequency range ensures high-speed data transfer, making the antenna well-suited for integration into advanced wearable devices. The circularly polarized (CP) radiation is generated using an optimized cross-slot feeding structure, which excites two orthogonal modes within the dielectric resonator [31,32]. The cross-slot is strategically placed in the feed to create the necessary phase difference between the modes, resulting in the generation of CP radiation. This approach ensures that the antenna provides improved signal reception and transmission, which is crucial for wearable applications where the orientation of the device may change frequently. The use of a cross-slot also enhances the bandwidth of the antenna, ensuring reliable performance over a wide range of operating frequencies.

To evaluate the performance of the finger-ring DRA, simulations are conducted using CST Microwave Studio, a leading electromagnetic simulation tool. The antenna is modeled under both free-space and on-body conditions, using an equivalent finger model to simulate real-world scenarios. This comprehensive simulation approach ensures that the antenna's performance is optimized for practical wearable applications, taking into account the interaction with the human body and ensuring stable operation in dynamic conditions. The simulation used the equivalent properties of human body tissues, specifically skin, fat, and muscle as shows in Table 2, and as reported in [33–36], that to evaluate the antenna performance on the finger of a human.

**Table 2.** Material Properties of Skin, Fat, and Muscle.

Property	Skin	Fat	Muscle
Permittivity ( $\epsilon_r$ )	19	6.51	27.4
Density ( $\text{kg/m}^3$ )	1109	911	1090
Conductivity (S/m)	22.8	4.42	29.4

### 3. Results

The return loss characteristics of the proposed finger-ring DRA are presented in Figure 3. These characteristics highlight the antenna's performance in terms of impedance matching and bandwidth. In free-space conditions, the antenna exhibits an impedance bandwidth of approximately 20%, which is a favorable value for maintaining efficient radiation and low reflection over the desired frequency range of 20–30 GHz. This bandwidth ensures that the antenna can operate effectively over a wide range of frequencies within the specified operating band, supporting high-data-rate communications. However, when the antenna is placed on the body, the impedance bandwidth is observed to decrease to 15%. This reduction is primarily due to the dielectric loading effect caused by the finger. When the antenna is in close proximity to the human body, the permittivity of the body influences the electromagnetic fields, altering the effective dielectric constant and resulting in changes to the resonant frequency and bandwidth of the antenna. The human body's higher permittivity causes a shift in the antenna's resonant frequency, typically causing a slight reduction in the operating frequency. This frequency shift is attributed to the change in effective permittivity of the antenna system when exposed to the body. The interaction with the body changes the propagation characteristics of the electromagnetic waves, influencing the impedance matching and resonance. While this effect slightly reduces the impedance bandwidth, the antenna still maintains stable performance with acceptable return loss values, demonstrating its viability for wearable applications.

The use of circular polarization in wearable antennas is particularly advantageous, as it minimizes polarization mismatch caused by arbitrary orientations of the device on the body, ensuring reliable communication and enhanced performance in dynamic environments [35,36]. The circular polarization (CP) performance of the proposed finger-ring DRA is evaluated through the axial ratio (AR), with the

results shown in Figure 4. The axial ratio is a key parameter for determining the quality of the circular polarization, with an ideal axial ratio of 1 corresponding to perfect circular polarization. In free-space conditions, the antenna exhibits a CP bandwidth of approximately 12%, which is indicative of a wide operating range where the circular polarization is maintained with minimal distortion.

This broad CP bandwidth ensures that the antenna can effectively support diverse communication scenarios, providing robust performance across the 20–30 GHz frequency range. However, in the on-body scenario, the CP bandwidth decreases significantly to 3.5%. This degradation in CP performance is primarily due to increased surface wave interactions and impedance mismatching caused by the proximity of the human body. Despite this reduction, the antenna still maintains acceptable performance for wearable applications, with the axial ratio remaining within the acceptable range for reliable communication.

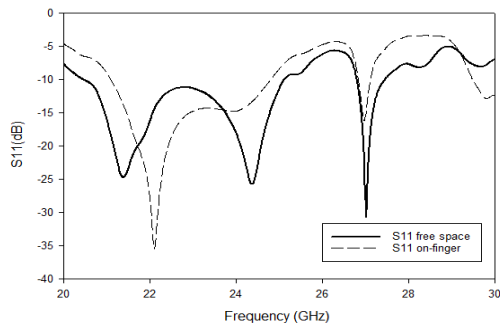


Figure 3. Ring  $S_{11}$  of ring DRA in free space and on-body.

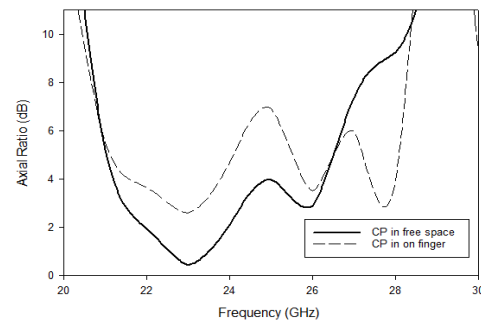


Figure 4. Ring CP in free space and on-body.

The peak gain of the proposed finger-ring DRA is measured to be approximately 8 dBi in free-space conditions, as shown in Figure 5. This high gain value is indicative of the antenna's ability to efficiently radiate energy in the desired direction, providing effective coverage for communication. However, when the antenna is placed in the on-body configuration, the peak gain decreases by about 1 dB. This reduction in gain is expected due to the interaction between the antenna and the human body, which introduces additional losses and alters the radiation pattern. Despite this decrease, the antenna maintains a relatively high gain in the on-body scenario, demonstrating its robustness for wearable applications.

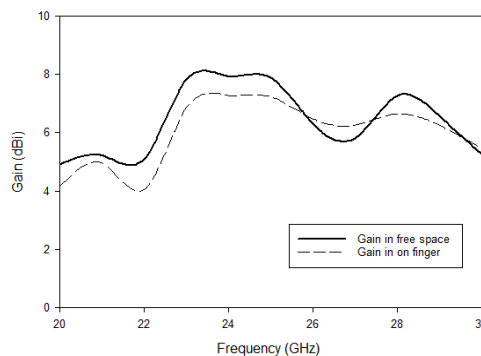


Figure 5. Ring Gain in free space and on-body.

The far-field radiation patterns of the antenna in both the E-plane and H-plane are shown in Figure 6, confirming that the antenna exhibits broadside radiation characteristics. In both planes, the radiation is primarily directed perpendicular to the surface of the antenna, ensuring efficient propagation in the desired direction. These broadside radiation patterns are essential for wearable applications, where maintaining consistent radiation characteristics regardless of the antenna's orientation is crucial. Despite the reduced gain in the on-body scenario, the radiation efficiency of the antenna remains above 85%, even with the presence of the human body. This high radiation efficiency indicates that the antenna is capable of effectively transferring the radiated energy into free space, minimizing losses due to the

body interaction. The robustness of the proposed design is thus confirmed, as it maintains high performance in terms of gain and efficiency, even when integrated into practical wearable systems.

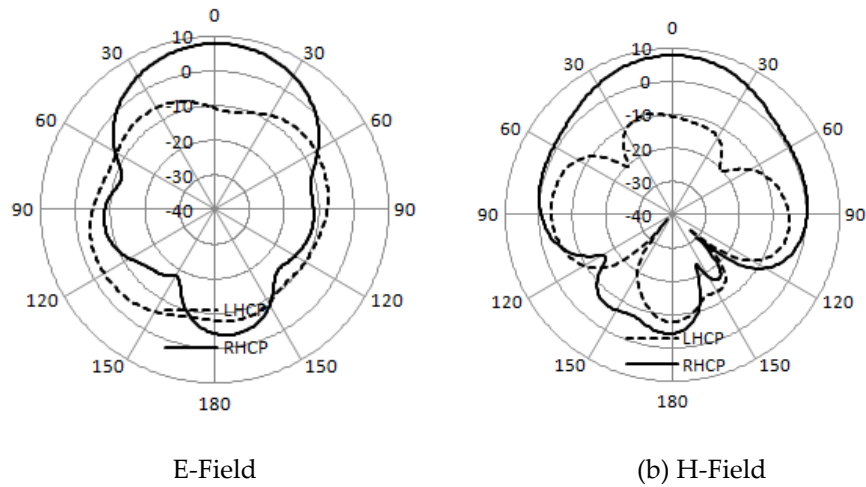


Figure 6. Radiation patterns at 24GHz.

#### 4. Discussion

Table 3 presents a comparative analysis of the proposed finger-ring DRA against literature-reported designs for similar wearable antenna configurations. This comparison highlights the performance characteristics, demonstrating the advantages of the proposed design in several key areas. The proposed ring DRA operates in the 20–30 GHz frequency range, designed specifically for finger-worn applications. It has an inner radius of 10 mm, which allows it to maintain a compact form factor while achieving a bandwidth (BW) of approximately 15%, which is a notable improvement over comparable design.

The gain of the proposed DRA is measured at 7.52 dBi, offering superior performance compared to other finger-worn antennas. Additionally, the circular polarization (CP) bandwidth of the proposed antenna is 3.5%, which, although lower than the free-space scenario, remains a viable value for wearable applications. In contrast, the Circular Phased Antenna Array in the literature, which also operates in the finger-worn configuration and at a 28 GHz operating frequency, has a gain of 5 and a CP bandwidth of linear polarization, indicating a lack of circular polarization, which limits its performance in dynamic environments. Moreover, the bandwidth of the phased antenna array is significantly lower, at 3.5%, suggesting that the proposed DRA outperforms it in terms of both gain and impedance bandwidth. Overall, the comparative analysis shows that the proposed finger-ring DRA offers superior gain and impedance bandwidth compared to similar designs, while maintaining a compact footprint, making it a promising candidate for practical wearable applications.

Table 3. Comparative analysis of the proposed finger-ring DRA against literature-reported.

Ref.	Frequency Band	Antenna Type	Key Features	Peak Gain
[21]	5 GHz	Microstrip Patch	-10 dB bandwidth: 90.3 MHz, Body-centric wireless sensor networks	6.9 dBi
[22]	902 MHz – 3.8 GHz	Conformal Loop	Covers ISM, LTE, WiMAX, 5G; indoor range >8.6m	-16.1 dBi at 2.45 GHz
[23]	7.25–10.25 GHz	Double Finger-Ring	UWB, minimal human finger interference	Not specified
[24]	2.45 GHz	Miniaturized Patch	Low SAR, compact size, medical sensing	Not specified

[25]	2.4–2.5 GHz, 915–930 MHz	Inverted-F	Evaluates position and rotation effects	Not specified
[26]	UHF RFID Band	RFID Tag	Read distance: 2–5m, Secure healthcare applications	Not specified
[27]	28 GHz	Microstrip Patch Array	mmWave 5G, compact structure	5.14 dB
Proposed Work	20–30 GHz	Circularly Polarized DRA	CP bandwidth: 12% (free-space), 3.5% (on-body); Peak gain ~8 dBi	8 dBi (off- body), ~7 dBi (on-body)

The proposed finger-ring antenna offers significant advantages over previous designs. Unlike prior works that focus mainly on microstrip or inverted-F antennas, this design utilizes a dielectric resonator antenna (DRA), which enhances radiation efficiency and polarization purity. The achieved wide CP bandwidth (12% in free-space, 3.5% on-body) surpasses many existing designs, especially in the mmWave spectrum. Furthermore, the higher gain (8 dBi off-body, ~7 dBi on-body) ensures robust communication performance, making this design a strong candidate for next-generation wearable wireless applications.

## 5. Conclusions

In this work, a conformal finger-ring Dielectric Resonator Antenna (DRA) has been successfully designed and analyzed for mm-wave wearable applications. The antenna demonstrates excellent performance, including a wide impedance bandwidth, circular polarization (CP), and stable gain in both free-space and on-body conditions. These attributes make it a promising candidate for integration into wearable systems operating at mm-wave frequencies, which are essential for high-speed communication in modern wireless technologies. The antenna's CP bandwidth in free-space is measured at 12%, but this bandwidth decreases to 3.5% in the on-body configuration due to the dielectric loading effects from the human body. While this reduction is expected in wearable designs, the performance of the antenna remains superior compared to existing finger-worn antennas in the literature. Specifically, the proposed DRA offers higher gain and larger impedance bandwidth, even with the body's interference, showcasing its robustness for wearable applications. Overall, this work lays a solid foundation for the development of compact, wearable mm-wave antenna systems that can be integrated into next-generation wireless communication devices. Future work can build upon these findings to optimize the antenna for more specific wearable applications, taking into account varying body positions and potential material innovations to further enhance performance.

**Author Contributions:** Author has contributed significantly to the development and completion of this article.

**Funding:** This article received no external funding.

**Data Availability Statement:** Not applicable.

**Acknowledgments:** The authors would like to express their sincere gratitude to Electrical and Electronic Engineering Department, Higher Institute of Engineering Technology-Tripoli, Libya, and School of Computer and Electronic Engineering (CSEE)University of Essex, UK, for their invaluable support and resources throughout the course of this research.

**Conflicts of Interest:** The author(s) declare no conflict of interest.

## ORCID

Tarek S Abdou <https://orcid.org/0009-0004-5469-5538>

Rawad Asfour <https://orcid.org/0009-0007-9381-4087>

## References

- [1] G. Chittimoju and U. D. Yalavarthi, "A comprehensive review on millimeter waves applications and antennas," *J. Phys.: Conf. Ser.*, vol. 1804, no. 1, p. 012205, Feb. 2021.

- [2] G. Federico, D. Caratelli, G. Theis, and A. B. Smolders, "A Review of Antenna Array Technologies for Point-to-Point and Point-to-Multipoint Wireless Communications at Millimeter-Wave Frequencies," *Int. J. Antennas Propag.*, vol. 2021, p. 5559765, 2021.
- [3] G. Kim and S. Kim, "Design and analysis of dual polarized broadband microstrip patch antenna for 5G mmWave antenna module on FR4 substrate," *IEEE Access*, vol. 9, pp. 64306–64316, 2021.
- [4] M. E. Munir et al., "A new mm-wave antenna array with wideband characteristics for next generation communication systems," *Electronics*, vol. 11, no. 10, p. 1560, 2022.
- [5] J. Khan et al., "Design of a millimeter-wave MIMO antenna array for 5G communication terminals," *Sensors*, vol. 22, no. 7, p. 2768, 2022.
- [6] K. Raheel et al., "E-shaped H-slotted dual band mmWave antenna for 5G technology," *Electronics*, vol. 10, no. 9, p. 1019, 2021.
- [7] M. Hussain et al., "Isolation improvement of parasitic element-loaded dual-band MIMO antenna for mm-wave applications," *Micromachines*, vol. 13, no. 11, p. 1918, 2022.
- [8] A. Bansal, C. J. Panagamuwa, and W. G. Whittow, "State-of-the-Art Millimeter-Wave Beam Steering Antennas for Beyond 5G and 6G Networks: A comprehensive review," *IEEE Antennas Propag. Mag.*, 2024.
- [9] O. Elalaouy, M. E. Ghzaoui, and J. Foshi, "A high-isolated wideband two-port MIMO antenna for 5G millimeter-wave applications," *Results Eng.*, vol. 23, p. 102466, 2024.
- [10] M. A. Haque et al., "Broadband high gain performance MIMO antenna array for 5G mm-wave applications-based gain prediction using machine learning approach," *Alexandria Eng. J.*, vol. 104, pp. 665–679, 2024.
- [11] U. Ali, S. Ullah, B. Kamal, L. Matekovits, and A. Altaf, "Design, analysis and applications of wearable antennas: A review," *IEEE Access*, vol. 11, pp. 14458–14486, 2023.
- [12] U. Musa et al., "Design and analysis of a compact dual-band wearable antenna for WBAN applications," *IEEE Access*, vol. 11, pp. 30996–31009, 2023.
- [13] M. Ikram, K. Sultan, M. F. Lateef, and A. S. Alqadami, "A road towards 6G communication—A review of 5G antennas, arrays, and wearable devices," *Electronics*, vol. 11, no. 1, p. 169, 2022.
- [14] S. Kiani, P. Rezaei, and M. Fakhr, "A CPW-fed wearable antenna at ISM band for biomedical and WBAN applications," *Wireless Netw.*, vol. 27, pp. 735–745, 2021.
- [15] C. Wang et al., "New Advances in Antenna Design toward Wearable Devices Based on Nanomaterials," *Biosensors*, vol. 14, no. 1, p. 35, 2024.
- [16] M. Wagih, G. S. Hilton, A. S. Weddell, and S. Beeby, "Millimeter-wave power transmission for compact and large-area wearable IoT devices based on a higher order mode wearable antenna," *IEEE Internet Things J.*, vol. 9, no. 7, pp. 5229–5239, 2021.
- [17] M. El Gharbi, R. Fernández-García, and I. Gil, "Embroidered wearable Antenna-based sensor for Real-Time breath monitoring," *Measurement*, vol. 195, p. 111080, 2022.
- [18] G. K. Soni, D. Yadav, and A. Kumar, "Flexible and wearable antenna design for Bluetooth and Wi-Fi application," *Int. J. Electr. Electron. Res.*, vol. 12, special issue, pp. 34–39, 2024.
- [19] S. Saleh, T. Saeidi, N. Timmons, and F. Razzaz, "A comprehensive review of recent methods for compactness and performance enhancement in 5G and 6G wearable antennas," *Alexandria Eng. J.*, vol. 95, pp. 132–163, 2024.
- [20] R. Joshi, "The Role of Wearable Antennas in Enhancing the Functionality of Wearable Devices," *Int. J. Antennas Propag.*, vol. 12, no. 1, Jan.–Feb. 2025.
- [21] W. Farooq et al., "Design of a finger ring antenna for wireless sensor networks," in *Proc. Eur. Conf. Antennas Propag. (EuCAP)*, Apr. 2016, pp. 1–4.
- [22] R. Alrawashdeh, "A wearable finger-ring antenna for smart-home Internet of Things," *Przegląd Elektrotech.*, no. 7, 2024.
- [23] H. Goto and H. Iwasaki, "A low profile double finger ring antenna for BAN and PAN," in *Proc. ISAP2010*, 2010.

- [24] R. Rabhi, A. Gharsallah, and O. M. Ramahi, "A miniaturized Wearable Finger-Ring Antenna For Medical Sensing at 2.45 GHz ISM Band," in *Proc. IEEE Int. Symp. Antennas Propag. USNC-URSI Radio Sci. Meeting, Jul. 2023*, pp. 1261–1262.
- [25] N. Noda and H. Iwasaki, "Evaluation related to finger position and rotation of wearable dual band inverted-F finger ring antenna," in *Proc. Int. Symp. Antennas Propag. (ISAP)*, Nov. 2015, pp. 1–4.
- [26] P. S. Taylor and J. C. Batchelor, "Finger-worn UHF far-field RFID tag antenna," *IEEE Antennas Wireless Propag. Lett.*, vol. 18, no. 12, pp. 2513–2517, 2019.
- [27] Z. Shuai and M. H. Sagor, "Wearable Finger Ring Antenna Array for 5G/mmWave Applications," in *Proc. IEEE Int. Conf. Telecommun. Photon (ICTP)*, Dec. 2019, pp. 1–3.
- [28] T. S. Abdou, R. Saad, and S. K. Khamas, "A circularly polarized mmWave dielectric-resonator-antenna array for off-body communications," *Appl. Sci.*, vol. 13, no. 3, p. 2002, 2023.
- [29] T. S. Abdou and S. K. Khamas, "A Multiband Millimeter-Wave Rectangular Dielectric Resonator Antenna with Omnidirectional Radiation Using a Planar Feed," *Micromachines*, vol. 14, no. 9, p. 1774, 2023.
- [30] A. I. Imran, T. A. Elwi, and A. J. Salim, "On the distortionless of UWB wearable Hilbert-shaped metamaterial antenna for low energy applications," *Progress In Electromagnetics Research M*, vol. 101, pp. 219–239, 2021.
- [31] A. A. Abdulmajid, S. Khamas, and S. Zhang, "Wide bandwidth high gain circularly polarized millimeter-wave rectangular dielectric resonator antenna," *Prog. Electromagn. Res. M*, vol. 89, pp. 171–177, 2020.
- [32] J. H. Lin, W. H. Shen, Z. D. Shi, and S. S. Zhong, "Circularly polarized dielectric resonator antenna arrays with fractal cross-slot-coupled DRA elements," *Int. J. Antennas Propag.*, vol. 2017, no. 1, p. 8160768, 2017.
- [33] T. S. Abdou and S. K. Khamas, "A Low-profile Wide Bandwidth Circularly Polarized Dielectric Resonator Antenna for mm-wave Off-Body Applications," in *Proc. Eur. Conf. Antennas Propag. (EuCAP)*, Mar. 2023, pp. 1–5.
- [34] P. Hasgall, F. Di Gennaro, C. Baumgartner, E. Neufeld, M. Gosselin, D. Payne, A. Klingensböck, and N. Kuster, "IT'IS Database for thermal and electromagnetic parameters of biological tissues," Version 2.6, Jan. 13, 2015. Available: [www.itis.ethz.ch/database](http://www.itis.ethz.ch/database). Accessed: Feb. 10, 2025.
- [35] A. Sabban, "Wearable circular polarized antennas for health care, 5G, energy harvesting, and IoT systems," *Electronics*, vol. 11, no. 3, p. 427, 2022.
- [36] Y. Chen, X. Liu, Y. Fan, and H. Yang, "Wearable wideband circularly polarized array antenna for off-body applications," *IEEE Antennas and Wireless Propagation Letters*, vol. 21, no. 5, pp. 1051–1055, 2022.



**Open Access** This article is licensed under a Creative Commons Attribution 4.0 International License, which permits use, sharing, adaptation, distribution and reproduction in any medium or format, as long as you give appropriate credit to the original author(s) and the source, provide a link to the Creative Commons licence, and indicate if changes were made. The images or other third-party material in this article are included in the article's Creative Commons licence, unless indicated otherwise in a credit line to the material. If material is not included in the article's Creative Commons licence and your intended use is not permitted by statutory regulation or exceeds the permitted use, you will need to obtain permission directly from the copyright holder. To view a copy of this licence, visit <http://creativecommons.org/licenses/by/4.0/>.